Truncated Human βB1-Crystallin Shows Altered Structural Properties and Interaction with Human βA3-Crystallin[†]

K. Srivastava,[‡] R. Gupta,[‡] J. M. Chaves,[‡] and O. P. Srivastava*

Department of Vision Sciences, University of Alabama at Birmingham, Birmingham, Alabama 35294 [‡]*These authors have equally contributed to the work presented.*

ABSTRACT: The purpose of the study was to determine the effects of truncation of various regions of βB1-crystallin on its structural properties and stability of heterooligomers formed by wild-type (WT) βB1 or its deletion mutants with WT βA3-crystallin. For these analyses, seven deletion mutants of βB1-crystallin were generated with the following sequential deletions of either N-terminal arm [βB1(59−252)], N-terminal arm + motif I [βB1(99−252)], N-terminal arm + motif I + motif II [βB1(144−252)], N-terminal arm + motif II + connecting peptide [βB1(149−252)], C-terminal extension [βB1(1−234)], C-terminal extension plus motif IV [βB1(1−190)], or C-terminal extension + motif III + motif IV [βB1(1−148)]. The βB1-crystallin became water insoluble on the deletion of C-terminal extension and subsequent deletions of the C-terminal domain (C-terminal extension plus motifs III and IV) while it remained partially soluble on the deletion of the N-terminal domain (N-terminal arm plus motifs I and II). However, circular dichroism spectral analysis showed that the deletion of the N-terminal domain but not the C-terminal domain exhibited relatively greater structural changes in the crystallin. The deletion of the C-terminal domain resulted in a greater exposure and disturbance in the microenvironment of Trp-100, Trp-123, and Trp-126 (localized in the motif II), suggesting a relatively greater role of the C-terminal domain than the N-terminal domain in the structural stability of the crystallin. The deletion of the N-terminal extension in βB1 resulted in maximum exposure of hydrophobic patches and compact structure and in a maximum loss of subunit exchange with WT βA3-crystallin compared to deletion of either the C-terminal extension, the N-terminal domain, or the C-terminal domain. The thermal stability results of the heterooligomer of βB1- plus βA3-crystallins suggested that oligomers lose their stability on deletion of the C-terminal domain. Together, the results suggested that the N-terminal arm of βB1-crystallin plays a major role in interaction with βA3-crystallin during heterooligomer formation, and the solubility of βB1-crystallin *per se* and that of the heterooligomer with βA3-crystallin are dependent on the intact C-terminal domain of βB1-crystallin.

The structural proteins (α-, β-, and γ-crystallins) provide transparency and refractive power to a vertebrate lens by virtue of their high concentrations and specific interactions. Among the crystallins, α- and β-crystallins are oligomeric while only γ-crystallin is monomeric. The α-crystallin is composed of two primary gene products (αA- and αB-crystallins), and the β−γ superfamily is constituted by four acidic (βA1, βA2, βA3, and βA4) and three basic (βB1, βB2, and βB3) β-crystallins and six γ-crystallins (γA, γB, γC, γD, γE, and γF) (1−4). Although the present literature suggests that β-crystallin oligomers play a critical role in the maintenance of lens transparency, the exact

interactions among the acidic and basic β-crystallins to form oligomers are largely unknown. In adult human lenses, the oligomers of β-crystallin are separated into βH (∼200 kDa)[1] and βL (∼40 kDa) fractions during size-exclusion chromatography, but an intermediate oligomer (βL1) between βH and βL also appears at about 1 year of age (5, 6). A previous study (5) identified three β-crystallin oligomers in human lenses, i.e., β1 (150 kDa), β2 (92 kDa), and β3 (46 kDa). The β1 oligomer contained βA3/A1-, βA4-, βB1-, and βB2-crystallins, the β2 oligomer contained βA3/A1-, βA4-, βB1-, and βB2-crystallins, and the β3 oligomer contained βB1- and βB2-crystallins. This study concluded that the major differences in the three oligomers were the presence of βA3/A1- and βA4-crystallins in the β1 and

[1]Abbreviations: ANS, 8-anilino-1-naphthalenesulfonate; Da, daltons; DTT, dithiothreitol; IPTG, isopropyl β-ᴅ-1-thiogalactopyranoside; MALDI-TOF, matrix-assisted laser desorption/ionization time of flight; SDS−PAGE, sodium dodecyl sulfate−polyacrylamide gel electrophoresis; EDTA, ethylenediaminetetraacetic acid.

Table 1: Oligonucleotide Primers of WT-βB1 and Its Mutants

WT and deletion mutant constructs		primers (5′−3′)
WT-βB1	forward	CACCATGTCTCAGGCTGCAAAGGCCTCGGCC
	reverse	TCACTTGGGGGGGCTCTGTGGCCAGGACAGG
βB1 (59−252)	forward	CACCTACAGGCTGGTGGTCTTCGAACTGG
	reverse	TCACTTGGGGGGGCTCTGTGGCCAGGACAGG
βB1 (99−252)	forward	CACCGGACCCTGGGTCGCCTTTGAGCAGTCC
	reverse	TCACTTGGGGGGGCTCTGTGGCCAGGACAGG
βB1 (144−252)	forward	CACCGATGCCCAGGAGCACAAAATCTCCCTG
	reverse	TCACTTGGGGGGGCTCTGTGGCCAGGACAGG
βB1 (149−252)	forward	CACCCACAAAATCTCCCTGTTTGAAGGGGCC
	reverse	TCACTTGGGGGGGCTCTGTGGCCAGGACAGG
βB1 (1−234)	forward	CACCATGTCTCAGGCTGCAAAGGCCTCGGCC
	reverse	GTCACGCAGGCGACGCAGGGACTGCATCTG
βB1 (1−190)	forward	CACCATGTCTCAGGCTGCAAAGGCCTCGGCC
	reverse	ACTGGAGACCTTCACGCTGCCCACGCGGTC
βB1 (1−148)	forward	CACCATGTCTCAGGCTGCAAAGGCCTCGGCC
	reverse	CTCCTGGGCATCCATTTTGATGGGCCGGAA

β2 oligomers and their absence in the βA3 oligomer, and the aggregate sizes correlated with the length of the N-terminal extension of βB1-crystallin. While this study identified interacting species among the three different β-crystallin oligomers in human lenses, it also suggested that the N-terminal arm of βB1-crystallins might play a role in the higher order oligomerization. In vivo, except for βB2-crystallin, which is present as a homodimer, other β-crystallins exist as heterodimers (*7*). For example, βB1 and βA3 spontaneously aggregate, and βB1/βA3 heterooligomers were found to be stable (*7−9*), and their CD spectra suggest that, following oligomerization, the two crystallins show secondary structural changes (*7*).

Among various β-crystallins, the three-dimensional X-ray structures of only βB1 and βB2 are presently known (*9, 10*). Both βB1- and βB2-crystallins consist of two tightly packed globular domains that are linked by a connecting peptide. Each of the two domains contains two Greek key motifs of antiparallel β-pleated sheets. The structures of βB1- and βB2-crystallins were analogous to the tertiary structure of γ-crystallins(*11*). However, unlike monomeric γ-crystallin, the acidic β-crystallins contain the N-terminal arm while the basic β-crystallins contain both the N-terminal arm and C-terminal extension. The potential roles of the N-terminal arm/C-terminal extension in oligomerization and stability of the oligomers are presently not fully understood and open to debate. Studies suggest that the intact N-terminal arm plays a key role in higher order assembly of human β_H-crystallin (*5, 9, 12−14*). The heterooligomers of βA3/βB1- and βA3/βB2-crystallin showed greater stability, and their interaction is believed to be essential for close packing of crystallins and, therefore, for the transparency of the lens (*15, 16*). Liu and Liang (*17*) showed that interactions among acidic and basic human β-crystallin were stronger than the acidic−acidic or basic−basic β-crystallins. The interaction also involves subunit exchange as suggested from results of heteromer formation between human βB1- and βA3-crystallins (*9, 13, 18*).

In a newborn human, the βB1-crystallin comprises 9% of the total crystallins (*2*), but with aging it undergoes several posttranslational modifications including truncation. In the newborn to 27 years of age in human lenses, the deletion of 15, 33, 34, 35, 36, 39, 40, and 41 amino acids in the N-terminal extension of βB1-crystallin is observed (*2*). This study also suggested that the partial degradation of the crystallin led to its insolubilization because both water-soluble and insoluble protein fractions of human lenses contained these species. Anomalous behavior of truncated forms of human βB1-crystallin (HβB1) missing the N-terminal 6, 14, 41, 43, 48, and 49 amino acid residues plus the C-terminal 12 residues was observed during gel permeation chromatography, which suggested their interaction with the column matrix and also self-association at higher concentrations (*18*). A comparison of properties of the βB1$\triangle$N41 protein with WT-βB1 suggested that truncation as a posttranslational modification favored protein condensation and the formation of light scattering elements (*12*). Similarly, deamidation of βB1 also altered its structural properties and interaction with βA3 during heterooligomerization (*15, 19, 20*). These reports mostly studied either truncation of the N-terminal arm or deamidation on structural properties of βB1-crystallin. The effects of truncations of motifs and/or the C-terminal extension on crystallin properties are yet to be determined. Similarly, as described above, although βB1- and βA3-crystallins readily form heterooligomers *in vitro*, the interacting regions of βB1- with βA3-crystallin are presently unknown. Therefore, our present study was focused on elucidation of effects of truncation of various regions of βB1-crystallin on its structural properties and identification of the the regions of βB1-crystallin that interact with βA3-crystallin. For this purpose, seven deletion mutants of βB1-crystallin were generated with sequential deletions of either the N-terminal arm (residues 1−58), N-terminal arm + motif I (residues 1−98), N-terminal arm + motif I + motif II (residues 1−143), N-terminal arm + motif I + motif II + connecting peptide (residues 1−148), C-terminal extension (residues 235−252), C-terminal extension plus motif IV (residues 191−252), or C-terminal extension + motif III + motif IV (residues 149−252). Using the above mutants, we determined the effects of deletions of specific regions on structural properties of βB1-crystallin and identified the regions of the βB1-crystallin that provide stable heterooligomers with WT βA3-crystallin.

EXPERIMENTAL PROCEDURES

Materials. The restriction endonucleases *Nhe*I and *Sac*II, the molecular weight protein markers, and DNA markers were purchased from either Amersham Biosciences (Piscataway, NJ) or Promega (Madison, WI). The T7 promoter, T7 terminator, and other primers used in the study were obtained from Sigma Genosis (St. Louis, MO). Unless indicated otherwise, all other

molecular biology grade chemicals used in this study were purchased from Fisher (Atlanta, GA) or Sigma (St. Louis, MO).

Bacterial Strains and Plasmids. The *Escherichia coli* BL21 (DE3) bacterial strain was obtained from Invitrogen (Carlsbad, CA). The human βB1-crystallin cDNA, cloned in a plasmid pCRTT/V5 TOPO vector, was received from Dr. Kirsten Lampi, Health Sciences University, Portland, OR. Cells were propagated in Luria broth, and recombinant bacteria were selected using ampicillin.

Site-Specific Mutagenesis. The human βB1 gene was sub-cloned into a pET100 directional TOPO vector to introduce a six-His tag. This was used as template with specific complementary primer pairs (Table 1) to generate the desired truncated βB1-crystallin mutants. The following mutants were generated using PCR-based mutagenesis: (i) βB1 (containing residues 59−252) (lacking N-terminal arm), (ii) βB1 (containing residues 99−252) (lacking N-terminal arm + motif I), (iii) βB1 (containing residues 144−252) (lacking N-terminal arm + motif I + motif II), (iv) βB1 (containing residues 149−252) (lacking N-terminal arm + motif I + motif II + connecting peptide), (v) βB1 (containing residues 1−234) (lacking C-terminal extension), (vi) βB1 (containing residues 1−190) (lacking motif IV + C-terminal extension), and (vii) βB1 (containing residues 1−148) (lacking motif III + motif IV + C-terminal extension). Briefly, 25 ng of template was used, and the PCR conditions were as follows: predenaturing at 95 °C for 5 min, followed by 30 cycles of denaturing at 95 °C for 30 s, annealing at 60−65 °C (depending on the T_m of the primers) for 30 s, and extensions at 72 °C for 1 min followed by a final extension at 72 °C for 10 min. The PCR products were ligated into the pET100 Directional TOPO vector (Invitrogen) using the manufacturer's instructions, and the positive clones were identified by restriction analysis using *Nhe*I and *Sac*II. The orientation of the DNA sequences was confirmed by their sequencing at the Core Facility of the University of Alabama at Birmingham.

Expression and Purification of Wild-Type and Mutant Proteins. *E. coli* BL21(DE3) was transformed with mutant amplicons using a standard *E. coli* transformation procedure as described previously (*21*). The proteins were overexpressed by addition of isopropyl β-D-1-thiogalactopyranoside (IPTG, final concentration of 1 mM), and the cultures were incubated further at 37 °C for 4 h. The cells were harvested and resuspended in lysis buffer [50 mM Tris-HCl (pH 8.0) containing lysozyme (0.25 mg/mL) and protease inhibitor cocktail (Sigma Chemicals)] and lysed by sonication at 5 °C. DNA was degraded using DNase I (10 μg/mL) and incubation on ice for 30 min. The soluble fraction was separated by centrifugation at 8000*g* for 15 min at 5 °C, and the pellet was resuspended in a detergent buffer (0.02 M Tris-HCl, pH 7.5, containing 1% (w/v) sodium deoxycholate, 0.2 M NaCl, and 1% NP-40) and centrifuged at 5000*g* for 10 min at 5 °C. The pellet was washed with 0.5% Triton X-100 (10 μg of DNase I was added if the pellet was viscous). The washing of the pellet was repeated as necessary to remove bacterial debris from the inclusion bodies. The pellet was resuspended in denaturation buffer [0.02 M sodium phosphate, pH 7.8, containing 8 M urea and 0.5 M NaCl (DB buffer)].

Purification of Wild-Type and Mutant Proteins. Depending on the expression of the desired mutant proteins in either the soluble fraction or the inclusion bodies, they were purified under either native or denaturing conditions as previously described (*21*). In case the desired protein was expressed in a partly soluble form (i.e., present in both the soluble fraction and inclusion bodies), the soluble protein fraction was selectively

used for its purification. All purification steps, including refolding of proteins, were carried out at 5 °C unless indicated otherwise. Each mutant protein contained six His tags and was purified by an affinity chromatographic method using a Pro-bond Ni^{2+} chelating column as described by the manufacturer (Invitrogen). Briefly, during purification under native conditions, a column was equilibrated with native buffer [NB buffer: 20 mM sodium phosphate (pH 7.8) containing 0.5 M NaCl], the protein preparation was applied to the column and then washed with NB containing 10 mM imidazole, and, finally, the matrix-bound protein was eluted with NB containing 250 mM imidazole (pH 7.8). During purification of a mutant protein under denaturing conditions, the column was equilibrated with DB buffer. Following protein application, the unbound proteins were eluted, first with DB buffer, which was followed by a second wash with DB buffer at pH 6.0 (pH adjusted with HCl) and a third wash with DB buffer at pH 5.3 (pH adjusted with HCl). The bound proteins were eluted with DB buffer (pH 7.8) containing 250 mM imidazole. SDS−PAGE analysis (*22*) was used to identify the fractions that contained the desired proteins during purification. Each protein purified under native conditions was pooled, dialyzed against 0.05 M phosphate buffer (pH 7.5) at 5 °C, and stored at −20 °C until used. The proteins purified under denaturing conditions were refolded as described below.

Refolding of Mutant Proteins Purified under Denaturing Conditions. The denatured mutant proteins were refolded in a urea-free buffer. Briefly, a desired protein was refolded by adding it dropwise to an excess of cold buffer (25 mM Tris-HCl, 1 mM DTT, pH 7.5) at 1:100 dilution (denatured protein:buffer). Far-UV circular dichroism spectra were recorded to determine whether a refolded WT βB1-crystallin protein had similar secondary structure as the native WT βB1-crystallin.

Determination of Structural Properties of WT βB1-Crystallin and Mutant Proteins. *(1) Circular Dichroism (CD) Studies*. To investigate the secondary structural changes in the WT-βB1 and its mutant proteins, their far-UV CD spectra were determined at room temperature using a JASCO spectropolarimeter, model 62DS. The βB1-crystallin preparations at 0.2−0.3 mg/mL (dissolved in 50 mM Tris-HCl, pH 7.9) were used for recording the far-UV CD spectra. The path length was 0.1 cm during the far-UV CD spectra determination. The spectra reported are the average of five scans, corrected for buffer blank and smoothed. Secondary structures were estimated using the SELCON program (*23*).

(2) Fluorescence Studies. All fluorescence spectra were recorded in corrected spectrum mode using a Shimadzu RF-5301PC spectrofluorometer with excitation and emission band passes set at 5 and 3 nm, respectively. The intrinsic Trp fluorescence intensities of the WT-βB1 and its mutants (0.15 mg/mL each), dissolved in 10 mM sodium phosphate buffer, pH 7.4, containing 100 mM NaCl, were recorded with an excitation at 295 nm and emission between 300 and 400 nm. Human WT βB1-crystallin contains a total of eight Trp residues, i.e., Trp-100, Trp-123, and Trp-126 in motif II, Trp-174 in motif III, Trp-192, Trp-215, and Trp-218 in motif IV, and Trp-236 in the C-terminal extension.

(3) ANS Binding Studies. The binding of a hydrophobic probe, 8-anilino-1-naphthalenesulfonate (ANS), to the WT-βB1 and mutant proteins was determined by recording fluorescence spectra after excitation at 390 nm and emission between 400 and 600 nm. In these experiments, 15 μL of 0.8 mM ANS (dissolved in methanol) was added to a protein preparation (0.15 mg/mL,
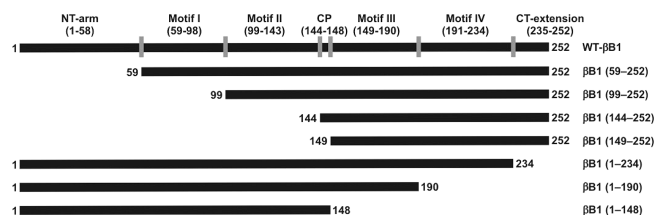
FIGURE 1: Schematic diagram to show the regions and residue numbers forming the N-terminal arm, N-terminal domain, C-terminal domain, and C-terminal extension in WT βB1-crystallin and its seven mutant proteins (identified by their names on the right). The following seven mutants were generated using PCR-based mutagenesis: (i) βB1 (59−252) (N-terminal arm truncated), (ii) βB1 (99−252) (N-terminal arm + motif I truncated), (iii) βB1 (144−252) (N-terminal arm + motif I + motif II truncated), (iv) βB1 (149−252) (N-terminal arm + motif I + motif II + connecting peptide truncated), (v) βB1 (1−234) (C-terminal extension truncated), (vi) βB1 (1−190) (C-terminal extension + motif IV truncated), and (vii) βB1 (1−148) (C-terminal extension + motif III + motif IV truncated).

dissolved in 10 mM phosphate buffer, pH 7.4). The samples were incubated at 37 °C for 15 min prior to their fluorescence measurements.

(4) Subunit Exchange Rates of WT βB1-Crystallin and Its Mutants with WT βA3-Crystallin. The rates of subunit exchange between βB1-crystallin (both WT and its mutants) and WT-βA3 were measured using the fluorescence resonance energy transfer (FRET) technique as described previously (21). WT βB1-crystallin and its mutants were labeled with Alexa fluor 350, and these acted as energy donors, while WT-βA3, labeled with Alexa fluor 488, acted as an energy acceptor. The fluorescent βB1−350 (WT or mutants) and WT-βA3−488 mixture was prepared in 1:1 ratio, and the subunit exchange was monitored at 37 °C in buffer A (50 mM sodium phosphate, pH 7.5, containing 100 mM sodium chloride and 2 mM DTT) for 2 h. The time-dependent decrease in donor fluorescence and concomitant increase in the acceptor fluorescence were monitored upon exciting the samples at the donor absorption maximum (346 nm). Curve fitting of the raw data using nonlinear regression analysis (using Sigma Plot 8.0 software) determined the subunit exchange rate.

To label the desired proteins, the manufacturer's recommended procedure (Molecular Probes) was used. Briefly, a desired protein was mixed with Alexa fluor dye in 50 mM sodium phosphate with 100 mM sodium bicarbonate. The reaction was allowed to proceed in the dark for 2 h at room temperature, and it was stopped by adding 1.5 M hydroxylamine, pH 8.5, and incubation for 1 h at room temperature. The excess of Alexa fluor dye was separated from the labeled proteins by dialyzing against 50 mM phosphate buffer at 5 °C for 48 h with two changes of the buffer using Spectra/Por membrane (molecular mass cutoff: 3500 Da).

(5) Oligomer Size Determination by Static Light Scattering. A multiangle laser light scattering instrument (Wyatt Technology, Santa Barbara, CA), coupled to a HPLC column (TSK gel 3000 PW$_{XL}$), was used to determine the absolute molar mass of homomers of WT-βB1 and its mutant proteins as well as heteromers of WT-βA3 plus WT-βB1 or its mutant proteins. Briefly, each protein sample was dialyzed in 29 mM Na$_2$HPO$_4$, 29 mM Na$_2$HPO$_3$, 100 mM KCl, 1 mM EDTA, and 1 mM DTT, pH 6.8, and mixed to generate heteromers, incubated at 37 °C for 90 min, and filtered through a 0.22 μm filter prior to their analysis. Results used 18 different angles, and the angles were normalized with the 90° detector. ASTRA V software (Wyatt

Table 2: Solubility of WT-βB1 and Its Mutant Proteins[a]

	soluble fraction	inclusion bodies
WT-βB1	+	+
βB1 (59−252)	+	+
βB1 (99−252)	−	+
βB1 (144−252)	+	+
βB1 (149−252)	+	+
βB1 (1−234)	−	+
βB1 (1−190)	−	+
βB1 (1−148)	−	+

[a] The (+) sign denotes the presence of the protein as observed on SDS−PAGE after centrifugation.

Technology) was used to determine molecular mass, distribution, and polydispersity of protein species.

(6) Thermal Stability of Complexes of WT-βA3 and WT-βB1 or Its Deletion Mutants. The thermal stabilities of complexes of WT-βA3 with WT-βB1 or its deletion mutants were determined as previously described by Lampi et al. (15). WT-βA3 and WT-βB1 or its deletion mutants were dialyzed against 29 mM Na$_2$HPO$_4$, 29 mM Na$_2$HPO$_3$, 100 mM KCl, 1 mM EDTA, and 1 mM DTT, pH 6.8, at 4 °C for 20 h. Next, these preparations were mixed at 1:1 ratio (0.1 mg of WT- βA3 and 0.1 mg of WT-βB1 or its deletion mutants) and heated to 55 °C for 3 h, and then turbidity was monitored at 405 nm every 5 min for 100 min while the samples were mixed every 5 min with a Pasteur pipet. In these analyses, the aggregation of the proteins was monitored at 405 nm (due to light scattering) as a function of time (100 min) using a scanning spectrophotometer (model UV2101 PC; Shimadzu, Columbia, MD) equipped with a six-cell positioner (model CPS-260; Shimadzu) and a temperature controller (model CPS 260; Shimadzu).

RESULTS

Expression and Purification of Human Recombinant WT-βB1 and Its Mutant Proteins from Soluble Fractions and/or Inclusion Bodies. As stated above, the human βB1 gene was subcloned into a pET100 directional TOPO vector to introduce a six-His tag and was used as template with specific complementary primer pairs (Table 1) to generate the desired deleted βB1-crystallin mutants. The human βB1-crystallin contains 252 residues, and it is composed of an N-terminal arm (residues 1−58), followed by two domains [N-terminal domain (residues 59−143) and C-terminal domain (residues 149−234)], connected by a short connecting peptide (residues 144−148) and a C-terminal extension (residues 235−252). Each of the domains contains two motifs [i.e., the N-terminal domain contains motif I (residues 59−98) and motif II (residues 99−143), and the C-terminal domain contains motif III (residues 149−190) and motif IV (residues 191−234)] (see Figure 1). As stated above in Experimental Procedures, we sequentially deleted βB1-crystallin beginning at the N-terminal arm, followed by each motif, and finishing at the C-terminal extension to generate the following seven deleted mutant (Figure 1) proteins: βB1 (59−252), βB1 (99−252), βB1 (144−252), βB1 (149−252), βB1 (1−234), βB1 (1−190), and βB1 (1−148).

Following the expression *in E. coli*, WT-βB1 was recovered in the soluble fractions, whereas βB1 (59−252), βB1 (144−252), and βB1 (149−252) were recovered in both the soluble and insoluble fractions. However, the βB1 (99−252), βB1 (1−234), βB1 (1−190), and βB1 (1−148) proteins were exclusively present in the
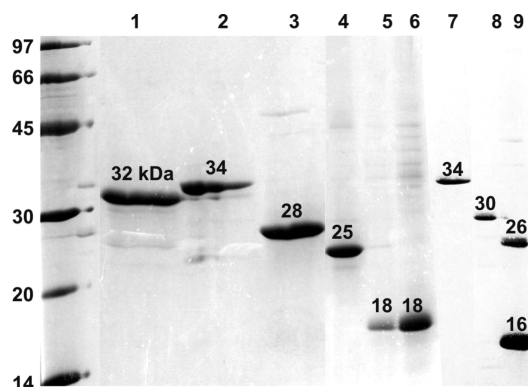
FIGURE 2: SDS−PAGE analysis of purified WT-βA3, WT-βB1, and its deletion mutant proteins. Lanes: 1, WT-βA3; 2, WT-βB1; 3, βB1 (59−252); 4, βB1 (99−252); 5, βB1 (144−252); 6, βB1 (149−252); 7, βB1 (1−234); 8, βB1 (1−190); 9, βB1 (1−148). Numbers above each band show their approximate molecular weight.

insoluble inclusion body fractions (Table 2). The mutant proteins present in soluble fractions were purified under native conditions, and those that were present in the insoluble fractions were purified under denaturing conditions using the Ni^{2+} affinity chromatographic method (*21*) as described in Experimental Procedures.

The DNA sequencing results confirmed desired deletions in the above mutants. To confirm the deletions in the expressed mutant proteins, individual protein bands with desired molecular masses were examined by the Q-TRAP mass spectrometric method following their excision from a SDS−PAGE gel (Figure 2). These analyses were performed using the desired protein species from crude *E. coli* preparations and also following purification of the WT βB1-crystallin and its mutant proteins as shown in Figure 2. The approximate molecular masses of the bands shown in Figure 2 were computed using the 1D-Gel Analysis module of ImageQuant TL 7.0 (GE Biosciences).

The proteins purified under denaturing conditions were refolded as described in Experimental Procedures. The purified WT and mutant proteins on SDS−PAGE analysis showed a single major protein band suggesting their highly purified nature (Figure 2). The WT and each mutant protein exhibited higher than expected molecular masses on SDS−PAGE analysis because they contained the tag with six His residues.

Comparison of Properties of WT βB1-Crystallin and Its Seven Truncated Mutant Proteins. *(1) Circular Dichroism Spectral Studies.* To evaluate the effects of deletion of different regions of βB1-crystallin on its structural properties, the far-UV CD spectra of the WT-βB1 and its mutant proteins were determined (Figure 3, Table 3). The WT βB1-crytsallin exhibited 14% α-helix, 55% β-sheet, 12% β-turn, and 18% random coil contents. In contrast, the N-terminal arm-deleted βB1 showed 26% α-helix, 53% β-sheet, 18% β-turn, and 4% random coil contents, suggesting the deletion of the N-terminal arm resulted in almost no change in β-sheet structure, a significant gain α-helix and β-turn, and reduced random coil structure. On deletion of the N-terminal arm plus motif I, the structural properties were similar to the WT βB1-crystallin, and the deletion of N-terminal arm plus motifs I and II showed increased random coil structure relative to the WT protein. However, on a complete deletion of the N-terminal domain plus connecting peptide (i.e., N-terminal arm plus motifs I and II and connecting peptide), the remaining C-terminal domain of βB1-crystallin showed a decrease in β-sheet content (44% compared to 55% in WT) and an increase in
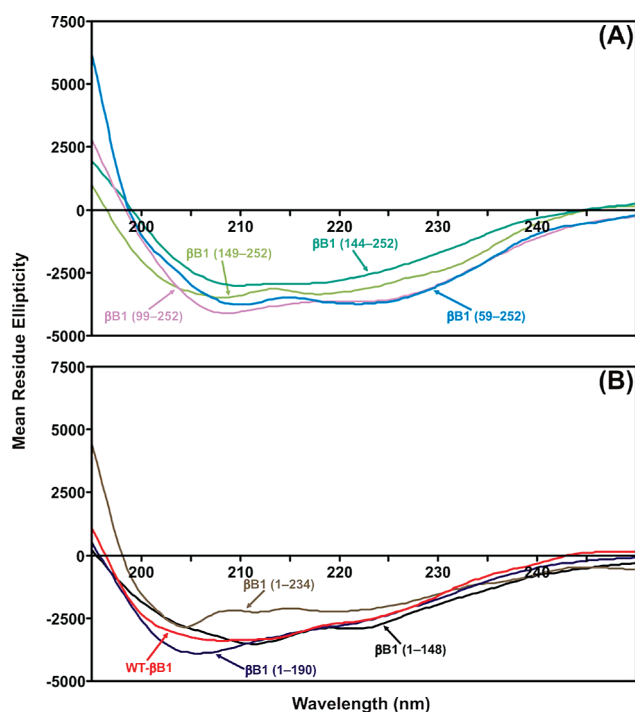

FIGURE 3: Far-UV CD spectra of WT-βB1 and its mutant proteins. The spectra were determined at room temperature using a JASCO spectropolarimeter, model 62DS. The βB1-crystallin preparations at 0.2−0.3 mg/mL (dissolved in 50 mM Tris-HCl, pH 7.9) were used for recording the far-UV CD spectra. The path length was 0.1 cm during the far-UV CD spectra determination. The spectra reported are the average of five scans, corrected for buffer blank, and were smoothed. Secondary structures were estimated using the SELCON program (*23*).

α-helical content (24% compared 14% in WT). The deletion of C-terminal extension dramatically increased the β-sheet structure (67% compared to 55% in WT), but deletion of the C-terminal domain (motifs III and IV) showed little change in structure. Together, the results showed that the deletion of the N-terminal arm plus N-terminal domain (motif I and II) showed greater influence on the structure of βB1-crystallin compared to the C-terminal domain (motifs III and IV). Further, the C-terminal domain was relatively more stable than the N-terminal domain in βB1-crystallin.

(2) Intrinsic Trp Fluorescence Spectra Studies. Human βB1-crystallin contains a total of eight Trp residues, i.e., Trp-100, Trp-123, and Trp-126 in motif II, Trp-174 in motif 3, Trp-192, Trp-215, and Trp-218 in motif IV, and Trp-236 in the C-terminal extension. On the basis of solvent accessibility and the X-ray structure of γ- and βB2 structures, Slingsby group (*8*) identified that Trp-100 and Trp126 of motif I and Trp-192 and Trp-218 of motif IV are buried and Trp-123, Trp-174, Trp-215, and Trp-236 are exposed. Therefore, upon the deletion of various regions of WT βB1-crystallin, the maximum changes in λ_{max} and the intensity of fluorescence at 340 nm (λ_{max} of WT) will occur because of exposure of buried Trp residues (Figure 4, Table 3). On deletion of the N-terminal arm, the λ_{max} was 341 nm, but the fluorescence in the mutant relative to the WT-βB1 increased. On deletion of the N-terminal arm plus motif I, a decrease in the fluorescence plus an increase in λ_{max} to 342 (a red shift) in the mutant was observed, suggesting that the microenvironment around buried Trp residues was affected. The deletion of the N-terminal arm + motifs I and II or the N-terminal arm + motifs I and II and connecting peptide resulted in loss of buried Trp-100,
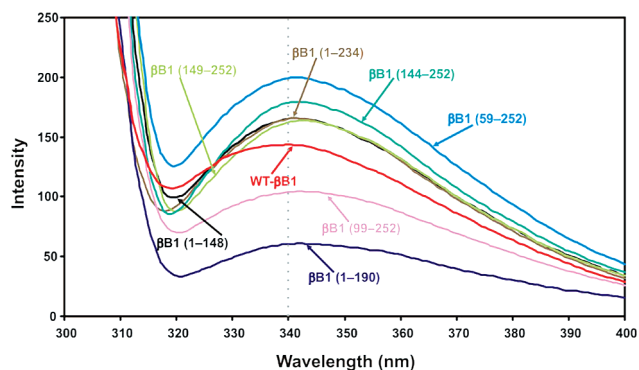
FIGURE 4: Intrinsic Trp fluorescence intensities of the WT-βB1 and its mutants. The proteins (0.15 mg/mL each) were dissolved in 10 mM sodium phosphate buffer, pH 7.4, containing 100 mM NaCl, and were recorded with an excitation at 295 nm and emission between 300 and 400 nm. Human βB1-crystallin contains a total of eight Trp residues, i.e., Trp-100, Trp-123, and Trp-126 in motif 2, Trp-174 in motif 3, Trp-192, Trp-215, and Trp-218 in motif 4, and Trp-236 in the C-terminal extension.
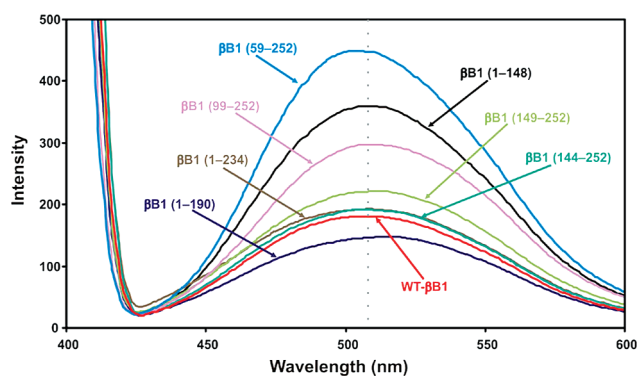

FIGURE 5: Binding of a hydrophobic probe, 8-anilino-1-naphthalenesulfonate (ANS), to the WT-βB1 and mutant proteins. In these experiments, 15 μL of 0.8 mM ANS (dissolved in methanol) was added to a protein preparation (0.15 mg/mL, dissolved in 10 mM phosphate buffer, pH 7.4). The samples were incubated at 37 °C for 15 min prior to recording fluorescence spectra after excitation at 390 nm and emission between 400 and 600 nm.

Trp-123, and Trp-126 residues, and the mutants showed a red shift (λ_{max} 342 and 343 nm, respectively) with an increased fluorescence relative to the WT protein. Therefore, these mutants had relaxed structures compared to the WT, and also suggested that these deletions resulted in altered microenvironments around the remaining Trp at Trp-174 in motif III, Trp-192, Trp-215, and Trp-218 in motif IV, and Trp-236 in the C-teminal extension. The deletion of C-terminal extension plus motif IV or C-terminal extension and motifs III and IV resulted in a red shift and change in the fluorescence. The data suggested that the deletion of motifs III and IV resulted in greater exposure of Trp-100, Trp-123, and Trp-126 in motif II that increased its fluorescence intensity and relaxed structure.

(3) Surface Hydrophobicity. To investigate the effects of truncations on surface hydrophobicity and the solvent-exposed nonpolar surfaces, the bindings of ANS to the WT-βB1 and its truncated mutant proteins were compared (Figure 5, Table 3). The ANS binding of mutant proteins relative to the WT βB1-crystallin was determined. On truncation of the N-teminal arm, the mutant protein exhibited increased ANS binding and blue shift to 504 nm, suggesting greater exposure of hydrophobic patches with relatively compact structure. On truncation of the
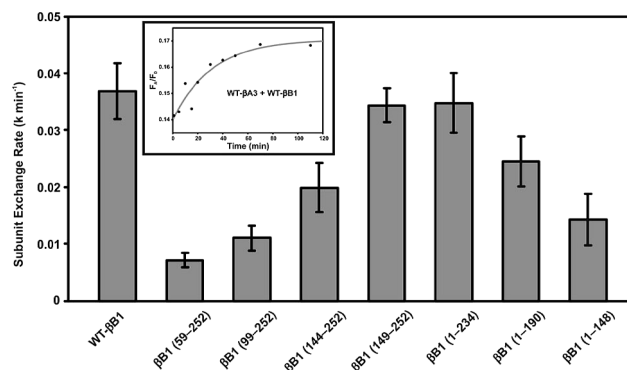

FIGURE 6: Subunit exchange rates between βB1-crystallin (WT or its mutants) and WT-βA3. The rates were measured using the fluorescence resonance energy transfer (FRET) technique. WT βB1-crystallin and its mutants were labeled with Alexa fluor 350, and these acted as energy donors, and WT-βA3, labeled with Alexa fluor 488, acted as an energy acceptor. The fluorescent βB1−350 (WT/mutant) and βA3−488 mixture was prepared in 1:1 ratio, and the subunit exchange was monitored at 37 °C in buffer A (50 mM sodium phosphate, pH 7.5, containing 100 mM sodium chloride and 2 mM DTT) for 2 h. The time-dependent decrease in donor fluorescence and concomitant increase in the acceptor fluorescence were monitored upon exciting the samples at the donor absorption maximum (346 nm). Curve fitting of the raw data using nonlinear regression analysis (using Sigma Plot 8.0 software) determined the subunit exchange rate. The inset shows the curve fitting (gray line) of the WT-βB1 and WT-βA3 mixture's raw data (black dots).

N-terminal arm plus motif I, the fluorescence intensity increased without any shift in its λ_{max}, suggesting little change in hydrophobic patches relative to the WT protein. On truncation of the N-terminal arm + motifs I and II, almost no change in both fluorescence intensity and λ_{max} was observed. In contrast, when the N-terminal arm plus N-terminal domain plus connecting peptide were deleted, the mutant protein exhibited a red shift to 512 nm with little increase in fluorescence intensity, suggesting a relatively relaxed structure but almost no greater exposure of the hydrophobic patches than WT-βB1. The deletion of the C-terminal extension exhibited a red shift and an increase in fluorescence intensity. Although a red shift was observed on deletion of the C-terminal extension plus motif IV, the fluorescence intensity decreased by almost 20%. However, the deletion of the C-extension + motifs III + IV exhibited little change in its λ_{max} but 2× higher fluorescence relative to the WT protein. Together, the results showed that relative to the WT protein the deletion of either the N-terminal arm or C-terminal domain (motif III + IV + C-terminal extension) resulted in increased exposure of hydrophobic patches.

(4) Subunit Exchange of WT-βB1 and Its Deletion Mutants with WT βA3-Crystallin during FRET Analysis. The subunit exchange rates between WT βB1-crystallin and its mutants with WT-βA3 were determined by the FRET technique as described previously (21). The rate of subunit exchange is shown in Table 4 and in Figure 6. The reduction in subunit exchange rates of WT βB1-crystallin and its mutants with WT βA3-crystallin occurred in the following order (from highest to lowest reduction): βB1 (59−252) > βB1 (99−252) > βB1 (1−148) > βB1 (144−252) > βB1 (1−190) > βB1 (149−252) ≥ βB1 (1−234). The results showed that deletion of the N-terminal arm in βB1-crystallin showed maximum decrease in its rate of subunit exchange with βA3-crystallin. Although deletion of the N-terminal domain (N-terminal arm + motif I and motif II) or C-terminal domain (motifs III and IV and C-terminal extension) of

Table 3: Structural Properties of WT-βB1 and Its Mutants

	CD spectra				Trp fluorescence	ANS binding		oligomerization	
	α-helix (%)	β-sheet (%)	β-turn (%)	random (%)	λ_{max} (nm)	λ_{max} (nm)	intensity (%)	molar mass (kDa)	approx subunits
WT-βB1	14.2	55.1	12.1	18.6	340.0	508.0	100.0	59.0 ± 1.8	2
βB1 (59−252)	25.7	53.1	17.6	3.6	341.0	504.0	248.0	75.5 ± 16.8	3
βB1 (99−252)	18.5	52.1	10.7	18.7	342.0	508.0	164.1	379.3 ± 14.2	20
βB1 (144−252)	13.4	54.3	10.3	22.0	342.0	507.0	105.9	11.6 ± 1.2	1
βB1 (149−252)	24.1	43.9	13.3	18.7	343.0	512.0	122.4	14.0 ± 3.1	1
βB1 (1−234)	8.7	67.3	8.0	16.0	341.0	509.0	106.0	9.9 ± 0.9	1
βB1 (1−190)	16.4	54.7	12.7	16.2	342.0	516.0	81.7	12240.0 ± 730.0	520
βB1 (1−148)	13.5	58.8	15.4	12.3	341.0	508.0	198.3	20.7 ± 2.7	1

Table 4: Interaction between WT-βA3 and WT-βB1 or Its Mutants at 1:1 Molar Ratio

	subunit exchange rate, k (min^{-1})	oligomerization, molar mass (kDa)	heat stability, protection[a] (%)
WT-βB1	0.0369 ± 0.0049	20.1 ± 1.1	83.76 ± 3.41
βB1 (59−252)	0.0072 ± 0.0013	67.9 ± 1.8	74.68 ± 2.99
βB1 (99−252)	0.0111 ± 0.0022	7.7 ± 0.7	98.81 ± 30.15
βB1 (144−252)	0.0199 ± 0.0043	22.9 ± 2.7	62.14 ± 2.73
βB1 (149−252)	0.0344 ± 0.0030	6.1 ± 0.3	81.07 ± 3.27
βB1 (1−234)	0.0348 ± 0.0052	10.6 ± 1.6	79.80 ± 3.60
βB1 (1−190)	0.0245 ± 0.0044	742.2 ± 97.7	65.22 ± 2.34
βB1 (1−148)	0.0143 ± 0.0045	5.3 ± 0.4	25.28 ± 2.58

[a] The protection of WT-βA3 from heat denaturation by WT-βB1 or its mutants at 1:1 molar ratio compared to the WT-βA3 alone (see Figure 7 inset).

Table 5: Oligomerization of Homomers (WT-βB1 or Its Mutants Alone) and Heteromers (WT-βA3 plus WT-βB1 or Its Mutants Mixed at 1:1 Molar Ratio)

	homomers				heteromers		
	distribution (%)	molar mass (kDa)	approx no. of subunits	polydispersity	distribution (%)	molar mass (kDa)	polydispersity
WT-βB1	54.8	59.0 ± 1.8	2	1.53 ± 0.24	54.5	20.1 ± 1.1	1.80 ± 0.16
	41.8	31.2 ± 0.8	1	1.02 ± 0.09	27.6	68.1 ± 1.1	1.09 ± 0.03
βB1 (59−252)	34.8	75.5 ± 16.8	3	1.00 ± 0.32	45.0	67.9 ± 1.8	1.11 ± 0.04
	22.0	196.2 ± 19.2	8	1.93 ± 0.33	25.2	11.3 ± 2.3	2.32 ± 0.94
βB1 (99−252)	27.5	379.3 ± 14.2	20	1.19 ± 0.03	47.7	7.7 ± 0.7	1.34 ± 0.16
	25.2	80.3 ± 4.8	4	1.70 ± 0.15	33.3	80.2 ± 1.6	1.03 ± 0.03
βB1 (144−252)	76.6	11.6 ± 1.2	1	1.03 ± 0.14	46.1	22.9 ± 2.7	1.98 ± 0.28
	10.9	58.9 ± 7.1	5	1.44 ± 0.34	41.7	220.9 ± 5.1	1.02 ± 0.03
βB1 (149−252)	86.6	14.0 ± 3.1	1	2.19 ± 0.89	62.4	6.1 ± 0.3	1.25 ± 0.08
	7.4	87.8 ± 26.7	6	7.67 ± 6.78	12.0	91.0 ± 2.4	1.16 ± 0.05
βB1 (1−234)	98.7	20.7 ± 2.7	1	12.46 ± 3.86	86.3	10.6 ± 1.6	1.60 ± 0.34
	1.0	90.1 ± 24.5	5	1.05 ± 0.39	7.4	68.5 ± 5.2	1.33 ± 0.14
βB1 (1−190)	43.2	12240.0 ± 730.0	520	1.01 ± 0.08	50.6	742.2 ± 97.7	1.07 ± 0.22
	32.4	692.2 ± 394.4	30	2.40 ± 1.90	26.1	7727.0 ± 615.0	1.47 ± 0.18
βB1 (1−148)	90.7	9.9 ± 0.9	0.5	5.35 ± 1.96	60.6	5.3 ± 0.4	1.96 ± 0.30
	4.1	132.0 ± 5.8	7	1.03 ± 0.06	24.4	63.2 ± 1.3	1.04 ± 0.03
WT-βA3	57.9	52.9 ± 0.8	2	1.08 ± 0.02	N/A	N/A	N/A
	24.4	6.6 ± 1.0	0.25	4.88 ± 1.74	N/A	N/A	N/A

βB1-crystalin exhibited lower subunit exchange rate with WT-βA3 than WT-βB1, it was higher than the mutant lacking the N-terminal arm [i.e., βB1 (59−252) mutant]. The data suggested that the N-terminal arm apparently has a major role in forming oligomers with βA3-crystallin. Nevertheless, motif I and the C-terminal extension plus motifs III and IV of βB1 also contributed in the oligomerization process with WT βA3-crystallin. Further, on deletion of the N-terminal arm plus N-terminal domain (motifs I and II) and the connecting peptide, the mutant βB1 (149−252) showed a higher rate of subunit exchange rate with WT-βA3, which was comparable to the rate of WT-βB1. This suggested that the C-terminal domain alone of βB1-crystallin could form heterooligomers with βA3-crystallin. Together, the results suggested that both N- and C-terminal domains of βB1-crystallin are capable of forming a heterooligomer with βA3-crystallin at varying degrees, which suggested multiple sites of WT-βB1 are in contact with WT-βA3 during oligomerization. However, the C-terminal domain of βB1 has a relatively more crucial role during such oligomerization.

(5) Determination of Molecular Mass by the Static Light Scattering Method. The molecular masses, polydispersities, distribution by mass, and the approximate number of subunits of WT-βA3, WT-βB1, and its mutant proteins are shown in Table 5 and in the summary table for homomers (Table 3). Similarly, the molecular masses, polydispersities, and distribution by mass of WT-βA3 plus WT-βB1 or its mutant

proteins (mixed at 1:1 molar ratio) are shown in Table 5 and the summary table for heteromers (Table 4). Note that although the molecular masses of more than one protein species that existed in homomers and heteromers are shown in Table 5, Tables 3 and 4 selectively show the molecular mass of the major protein species in these homomers and heteromers, respectively. About 55% of WT-βB1 was present as a polydispersed dimer (60 kDa), while 42% of it remained as a monomer (31 kDa). While 58% of WT-βA3 was present as a dimer (53 kDa). It formed a polydispersed monomer of about 20 kDa (55%) and an oligomer of about 68 kDa (28%) when mixed with WT-βB1. The N-terminal arm truncated βB1 mutant was present throughout a wide range of molecular masses, but most of it (35%) was present as a trimer (76 kDa), and 22% was present as an octamer (196 kDa). When mixed with WT-βA3, the resulting molecular masses are 68 and 11 kDa. The βB1 (99−252) mutant protein also showed a wide range of molecular masses, where a 380 kDa oligomer (28%) and a tetramer (25%) are the most abundant. When mixed with WT-βA3, βB1 (99−252) showed 8 kDa fragments and an 80 kDa oligomer. The βB1 (144−252) mutant, missing the entire N-terminal domain, was mostly present as a 14 kDa monomer (77%) and a 60 kDa pentamer. When combined with WT-βA3, the mutant forms a 23 kDa species (46%) and a 220 kDa oligomer. The N-terminal domain plus connecting peptide truncated mutant βB1 (149−252) showed mostly a 12 kDa monomer (87%) and a vastly polydispersed 88 kDa hexamer (7%). When combined with WT-βA3, 62% of the heteromer had a mass of only 6 kDa and 12% had a mass of 91 kDa. The C-terminal extension truncated mutant was extremely polydispersed with an average molar mass of 21 kDa. Its heteromer with WT-βA3 showed a molar mass of only 11 kDa (86%) and a molar mass of 69 kDa (7%). The βB1 (1−190) mutant protein aggregated to form 12240 (43%) and 692 (32%) kDa oligomers. After mixing it with WT-βA3, the heteromers formed had masses of 742 (51%) and 7727 (26%) kDa. Finally, the C-terminal domain deleted mutant showed a polydispersed molar mass averaging 10 kDa (91%) and a 132 kDa heptomer (4%). Its heteromer with WT-βA3 showed a 5 kDa fragment (61%) and a 63 kDa (24%) oligomer.

While the homomers of WT-βB1 and WT-βA3 are present mostly as dimers, their mixture leads to a rearrangement of subunits yielding a truncated monomer as well as an oligomer of about 70 kDa. However, little interaction was observed in the mixture of WT-βA3 and βB1 (59−252) since the molar masses observed are within the ranges of their homomers. Some interaction was present when mixing WT-βA3 and βB1 (99−252) as observed a 8 kDa fragment and a oligomer of 80 kDa, whose mass resembles that of βB1 (99−252)'s tetramer but might still be a heteromer formed by the subunit exchange of the respective homomers. The N-terminal domain deleted βB1 (144−252) mutant formed a truncated species and an oligomer with WT-βA3. These masses vary greatly from the original homomer. The heteromer of the C-terminal extension deleted βB1 and WT-βA3 showed a molar mass of half of that of the homomeric βB1 (1−234). Some interaction was observed between WT-βA3 and βB1 (1−190) since the heteromer aggregated to form an almost 8000 kDa, which was smaller than the 12000 kDa oligomer formed by homomers of the truncated βB1-crystallin. Limited interaction was observed between WT-βA3 and the C-terminal domain deleted mutant. The oligomers formed were fragments or barely bigger than the dimerized WT-βA3 observed in the WT-βA3 homomers but, as stated above, might still be a heteromer.
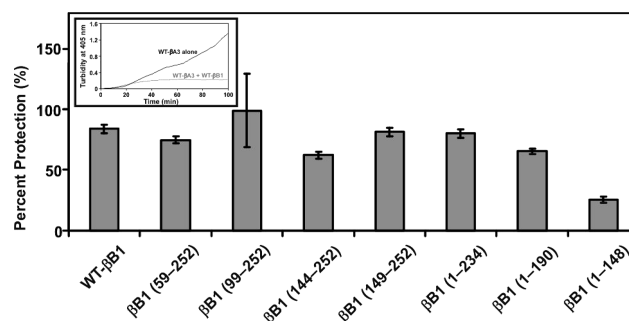

FIGURE 7: Thermal stability of complexes of WT-βA3 and WT-βB1 or its deletion mutants. The thermal stability was determined as previously described by Lampi et al. (*24*). The WT-βA3 and WT-βB1 or its deletion mutants were mixed at 1:1 ratio (0.1 mg of WT-βA3 and 0.1 mg of WT-βB1 or its deletion mutants) and heated to 55 °C for 3 h, and then turbidity was monitored at 405 nm every 5 min for 100 min while the samples were mixed every 5 min with a Pasteur pipet. In these analyses, the aggregation of the proteins (due to light scattering) as a function of time (100 min) was monitored using a scanning spectrophotometer (model UV2101 PC; Shimadzu, Columbia, MD) equipped with a six-cell positioner (model CPS-260; Shimadzu) and a temperature controller (model CPS 260; Shimadzu). The bar graph shows the percent protection exhibited by WT-βB1 and its mutants compared to denaturation of WT-βA3 alone. The inset shows the turbidity at 405 nm of WT-βA3 alone (black line) and WT-βA3 plus WT-βB1 (gray line).

The molecular masses for certain protein species were lower than expected because of their interaction with the column matrix, and therefore, the exact molecular mass could not be determined.

(6) Thermal Stability of Complexes of WT-βA3 and WT-βB1 or Its Deletion Mutants. While the FRET assay examined the subunit exchange rates between WT-βB1/its mutants and βA3-crystallin, the stability of their complexes was investigated by determining the heat stability. The thermal stability at 55 °C of heterooligomers of WT-βA3 with WT-βB1 or its deletion mutants is shown in Figure 7. The results are presented as relative protection of WT-βA3 on heating at 55 °C by WT-βB1 and its deletion mutants. The thermal stability of WT-βA3 on heating with WT-βB1 and βB1 (59−252), βB1 (99−252), βB1 (149−252), and βB1 (1−234) mutants was almost at the same levels. However, the thermal protection of βA3 was relatively lower in the presence of βB1 (144−252), βB1 (1−190), or βB1 (1−148) mutants, with dramatic loss in the stability in the presence of the βB1 (1−148) mutant protein. The results suggested that the heterooligomers that were formed on interaction of βB1-deletion mutants that lacked the N-terminal domain showed relatively greater thermal stability than those that lacked the C-terminal domain. This suggested that in the heterooligomers of βA3-crystallin and βB1-crystallin, the interaction of the C-terminal domain was needed to keep the protein in soluble and stable form.

DISCUSSION

The major findings of the study were as follows: (1) The βB1-crystallin became water insoluble on deletion of its C-terminal domain while on the deletion of the N-terminal domain, the protein was partially soluble. The results suggested that the C-terminal domain plays a significant role in the solubility of βB1-crystallin compared to the N-terminal domain. (2) The deletion of the N-terminal domain (N-terminal arm plus motifs I and II) of βB1-crystallin showed greater secondary structural changes than the deletion of the C-terminal domain (C-terminal extension

plus motifs III and IV). Therefore, contrary to the above contribution of the two domains in the βB1-crystallin solubility, the C-terminal domain showed relatively greater stability than the N-terminal domain. (3) The deletion of motifs III and IV resulted in greater exposure and disturbance in the microenvironment of Trp-100, Trp-123, and Trp-126 (localized in the motif II), as evident from an increase in fluorescence intensity and relaxed structure. These results were consistent with the above observation of relatively greater stability of the C-terminal domain than the N-terminal domain. (4) The deletion of the N-terminal arm resulted in maximum exposure of hydrophobic patches and compact structure compared to deletion of either the C-terminal extension, N-terminal domain (motifs I and II), or C-terminal domain (motifs III and IV). However, the C-terminal domain deleted βB1 mutant also exhibited increased exposure of hydrophobic patches compared to WT βB1-crystallin. (5) The deletion of the N-terminal arm in βB1-crystallin compared to other regional deletions showed a maximum loss in its subunit exchange with WT βA3-crystallin. While motif I and the C-terminal domain of βB1 also contributed to the oligomerization process, the results suggested that the N-terminal arm of βB1-crystallin plays a major role in forming heterooligomers with βA3-crystallin. (6) The thermal stability of the heterooligomer of βB1 plus βA3 results suggested that interaction of βA3 with the C-terminal domain compared to the N-terminal domain was of greater importance to keep the oligomer in a soluble and stable form. Further, the C-terminal domain deleted βB1 exhibited slower interaction with βA3, and their heterooligomers were less stable than that of WT-βB1 and WT-βA3. This is consistent with the above results showing a greater contribution of the C-terminal domain than the N-terminal domain in keeping βB1 in a soluble form. The subunit exchange and thermal stability experiments suggest that in spite of truncations in βB1 the resulting mutants with only partial structure of the crystallin were capable of interacting with βA3-crystallin. This could be due to recognition of specific sites of interaction among the two crystallins during *in vitro* incubation.

The protein−protein interaction plays a crucial role in maintaining lens transparency (*24*). As stated above, four acidic (βA1, βA2, βA3, and βA4) and three basic (βB1, βB2, and βB3) β-crystallins exist as oligomers in a vertebrate lens (*1−4*). Dimers of β-crystallins are believed to be the building blocks of their oligomers (*16, 17*), but presently the exact subunit compositions of oligomers and their mechanism of oligomerization remain poorly understood. Because βB1-crystallin is found in the β$_H$ crystallin fraction during size-exclusion chromatography, it is believed to interact with other β-crystallins in higher order assembly. A recent study concluded that acidic and basic β-crystallins show relatively stronger interactions compared to acidic−acidic or basic−basic β-crystallins (*17*). The interactions among individual β-crystallins are very specific because such interaction between βB1 with βA4-crystallins resulted in enhanced solubility of the latter (*25*) and, similarly, an enhanced solubility of βA2 on coexpression with βB2-crystallin (*26*). On the contrary, βA4 showed aggregates due to low solubility, which could not be solubilized on coexpression with βB2-crystallin (*26*). Together, the previous data clearly show the specificity of interactions among β-crystallins *in vivo* during oligomerization that lead to their solubility and lens transparency.

The crystal structure of human truncated βB1-crystallin at 1.4 Å resolution is known (*9*). Unlike βB2-crystallin structure (*10*), which showed domains swapping in homodimers, the βB1

homodimers showed intramolecular pairing of domains. Therefore, the structure of βB1-crystallin is close to γ-crystallin and structurally folds into N- and C-terminal domains with each containing two Greek key motifs. Each Greek key motif contains four consecutive β-strands that intercalate to form two β-sheets. The human γB- and γD-crystallin structures (*11, 27*) contain a central hydrophobic cluster and polar peripheral pairwise interactions surrounding the cluster.

In human βB1-crystallin, the intermolecular interactions, which stabilize its dimers and higher order assembly of the dimers, have been identified (*28*). In the βB1 monomer, Arg-232 of motif IV interacts with Asp-168 of motif III. In the higher molecular assembly of βB1 dimers, one βB1 dimer could interact with more than eight other dimers via two interfaces (*28*). In interface 1, the N-terminal arm and amino acids of the connecting peptide and C-terminal extension of one monomer interact with amino acids located on the N-terminal arm and motif III of the other monomer. In interface 2, amino acids located in motif II of one monomer interact with amino acids of motifs II and IV of the other monomer (*28*). Together, the data suggest multiple contact sites involving the N-terminal arm, C-terminal extension, and N- and C-terminal domains of βB1-crystallin during dimer formation and higher order assembly of βB1 dimers.

In the young human lenses, βB1 loses the N-terminal 15 amino acids and late 33 and 41 N-terminal amino acids during aging (*1, 2*). Lampi et al. also showed that the truncation of the N-terminal arm and C-terminal extension did not alter the stability of βB1-crystallin (*29*), which has been attributed to their flexible nature (*30*). The potential role of the N-terminal arm of βB1-crystallin is not well understood although its function as a facilitator for interaction of βB1 with other β-crystallins has been proposed (*5*). The results presented in this report show that relative to the WT protein the deletion of the N-terminal arm in βB1-crystallin increased both its α-helix content and exposure of hydrophobic patches and substantially reduced its subunit exchange rate with βA3-crystallin. Therefore, the N-terminal arm plays an important role in both maintaining βB1 structure and also in heterooligomer formation with βA3. The deletion of the C-terminal extension in βB1 increased the β-sheet contents but did not affect other properties such as exposure of hydrophobic patches and subunit exchange rate with βA3-crystallin. A βB1 mutant lacking the N-terminal 41 amino acids, which mimics *in vivo* degradation (*2*), has been studied first by Bateman et al. (*18*) and later by Annunziata et al. (*12*). The first study showed that while the full-length βB1-crystallin behaves like a dimer, this N-terminally truncated βB1 exhibited interaction with the column matrix and anomalous behavior during size-exclusion chromatography. Further, it was noted that an increasing degree of truncation of βB1 correlated with a greater retention by the column matrix. The second study (*12*) compared the CD spectra of the mutant lacking 41 amino acids of the N-terminal arm with WT βB1-crystallin and concluded that deletion did not result in major structural alterations. Based on additional results of this study, it was implied that the N-terminal arm in the native βB1-crystallin is extended outside of the globular domain and suppresses oligomerization and liquid−liquid phase separation and prevents protein crystallization (*12*). These conclusions are consistent with the proposed interaction sites identified during dimer and higher order oligomer formation by βB1-crystallin (*9*) and the results presented in our report.

During oligomerization of human βB2-crystallin, the interacting domains are β-sheets, and each β sheet is formed by two or

more β-strands. The X-ray refractive studies of the βB2-crystallin dimer showed that each subunit contain 16 β-strands and some of them play relatively greater roles in the dimer and higher order oligomerization process (*31*). Further, apparently the last three β-strands are involved in dimerization in βB1-crystallin (*31*). The potential involvement of β-strands in the dimerization of βB1-crystallin is presently unclear.

A surprising trend was seen between the hydrophobicity of βB1 and its mutants and their interactions with WT-βA3. The degree of exposed surface hydrophobic patches in βB1 and its mutants was inversely proportional to subunit exchange rates between them and βA3-crystallin. However, this relationship was observed to a lesser degree during thermal stability of their heterooligomers.

Our results provided evidence that the N-terminal arm of βB1-crystallin plays a major role in interaction with βA3-crystallin during heterooligomer formation, and the solubility of βB1-crystallin *per se* and that of heterooligomer with βA3-crystallin is dependent on the intact C-terminal domain of βB1-crystallin. The structural instability of βB1 was significantly increased on deletion of the C-terminal domain as evident from its insolubility and the lack of thermal stability of its oligomers with βA3-crystallin. A recent study of *ex vivo* incubation of mice lenses with gelatinase B resulted in cataract development (*32*), which was attributed to truncation of 47 N-terminal amino acids in βB1-crystallin with cleavage at the Ala_{47}–Lys_{48} bond. This study suggested that the loss of 47 N-terminal amino acids in βB1 causes reduced protein−protein interaction and insolubility. Similarly, a Q155X mutant of βB2 that lacked 51 C-terminal residues also showed decreased protein stability, altered conformation, and also reduced protein−protein interaction (*33*). Two large inbred Bedouin families from southern Israel showed an autosomal recessive form of congenital cataract, and the affected individuals of both families showed a frame shift mutation causing a missense protein sequence at amino acid 57 and truncation at amino acid 107 of βB1-crystallin (*34*).

Our studies demonstrate that the deletion of the N-terminal arm of βB1-crystallin resulted in maximum exposure of hydrophobic patches, compact structure, and also maximum loss in its subunit exchange rate with WT βA3-crystallin. However, an intact C-terminal domain is crucial for the solubility of βB1-crystallin and its oligomerization with βA3-crystallin. In this regard, the posttranslational modifications such as truncation of βB1-crystallin in specific N-terminal and/or C-terminal regions will lead to instability in its structure, loss of solubility, and reduced capability to form oligomers with other crystallins.

ACKNOWLEDGMENT

REFERENCES

1. Lampi, K. J., Ma, Z., Shih, M., Shearer, T. R., Smith, J. B., Smith, D. L., and David, L. L. (1997) Sequence analysis of βA3, βB3, and βA4 crystallins completes the identification of the major proteins in young human lens. *J. Biol. Chem. 272*, 2268–2275.
2. David, L. L., Lampi, K. J., Lund, A. L., and Smith, J. B. (1996) The sequence of human βB1-crystallin cDNA allows mass spectrometric detection of βB1 protein missing portions of its N-terminal extension. *J. Biol. Chem. 271*, 4273–4279.
3. Miesbauer, L. R., Smith, J. B., and Smith, D. L. (1993) Amino acid sequence of human lens βB2-crystallin. *Protein Sci. 2*, 290–291.
4. Bloemendal, H., deJong, W., Jaenicke, R., Lubsen, N. C., Slingsby, C., and Tardieu, A. (2004) Ageing and vision: structure, stability and function of lens crystallins. *Prog. Biophys. Mol. Biol. 86*, 407–485.
5. Azaz, M. S., Ma, Z., Smith, D. L., and Smith, J. B. (1997) Size of human lens β-crystallin aggregates are distinguished by N-terminal truncation of βB1. *J. Biol. Chem. 272*, 11250–11255.
6. Ma, Z., Hanson, S. R. A., Lampi, K. J., David, L. L., Smith, D. L., and Smith, J. B. (1998) Age-related changes in human lens crystallins identified by HPLC and mass spectrometry. *Exp. Eye Res. 67*, 21–30.
7. Jaenicke, R., and Slingsby, C. (2001) Lens crystallins and their microbial homologues: Structure, stability, and function. *Crit. Rev. Mol. Biol. 36*, 435–499.
8. Bateman, O. A., Sarra, R., van Genesen, S. T., Kappe, G., Lubsen, N. H., and Slingsby, C. (2003) The stability of human acidic β-crystallin oligomers and hetero-oligomers. *Exp. Eye Res. 77*, 409–422.
9. Chan, M. P., Dolinska, M., Sergeev, Y. V., Wingfield, P. T., and Hejtmancik, J. F. (2008) Associaition properties of beta B1-and beta A3-crystallins: Ability to form heterotetramers. *Biochemistry 47*, 11062–11069.
10. Bax, B., Lapatto, R., Nalini, V., Driessen, H. P. C., Lindley, P. F., Mahadevan, D., Blundell, T. L., and Slingsby, C. (1990) X-ray analysis of βB2-crystallin and evolution of oligomeric lens proteins. *Nature 347*, 776–780.
11. Najmudin, S., Nalini, V., Driessen, H. P. C., Slingsby, C., Blundell, T. L., Moss, D. S., and Lindley, P. F. (1990) Structure of the bovine eye lens protein γB(γII)-crystallin at 1.47 Å. *Acta Crystallogr., Sect. D 49*, 223–233.
12. Annunziata, O., Pande, A., Pande, J., Ogun, O., Lubsen, N. H., and Benedek, G. B. (2005) Oligomerization and phase transitions in aqueous solutions of native and truncated human βB1-crystallin. *Biochemistry 44*, 1316–1328.
13. Hejtmancik, J. F., Wingfield, P. T., and Sergeev, Y. V. (2004) Beta-crystallin association. *Exp. Eye Res. 79*, 377–383.
14. Hope, J. N., Chen, H. C., and Hejtmancik, J. F. (1994) Beta A3/A1-crystallin association: Role of the N-terminal arm. *Protein Eng. 7*, 445–451.
15. Takata, T., Woodbury, L. G., and Lampi, K. J. (2009) Deamidation alters interaction of β-crystallins in heterooligomers. *Mol. Vision 15*, 241–249.
16. Hejtmancik, J. F., Wingfield, P. T., Chambers, C., Russell, P., Chen, H. C., Sergeev, Y. V., and Hope, J. N. (1997) Association properties of βB2- and βA3-crystallin: ability to form dimers. *Protein Eng. 10*, 1347–1352.
17. Liu, B.-N., and Liang, J. J.-N. (2007) Protein-protein interactions among human lens acidic and basic β-crystallins. *FEBS Lett. 581*, 3936–3942.
18. Bateman, O. A., Lubsen, N. H., and Slingsby, C. (2001) Association behaviour of human βB1-crystallin and its truncated forms. *Exp. Eye Res. 73*, 321–331.
19. Lampi, K. J., Kim, Y. H., Bachinger, H. P., Boswell, B. A., Lindner, R. A., Carver, J. A., Shearer, T. R., David, L. L., and Kapfer, D. M. (2002) Decreased heat stability and oincreased chaperone requirement of modified human beta B1-crystallin. *Mol. Vision 8*, 359–366.
20. Takata, T., Oxford, J. T., Demeler, B., and Lampi, K. J. (2008) Deamidation destabilizes and triggers aggregation of a lens protein, beta A3-crystallin. *Protein Sci. 17*, 1565–1575.
21. Chaves, J. M., Srivastava, K., Gupta, R., and Srivastava, O. P. (2008) Effects of deletion of N- and C-terminal domains on human lens deamidated alpha A-crystallin. *Biochemistry 47*, 10069–10083.
22. Laemmli, U. K. (1970) Cleavage of structural proteins during the assembly of bacteriophage T4. *Nature 227*, 680–685.
23. Sreerama, N., Venyaminov, S. Y., and Woody, R. W. (1999) Estimation of number of alpha-helical and beta strand segments in proteins using circular dichroism spectroscopy. *Protein Sci. 8*, 370–380.
24. Takemoto, L., and Sorensen, C. M. (2008) Protein-protein interactions and lens transparency. *Exp. Eye Res. 87*, 496–501.
25. Marin-Vinader, L., Onnekink, C., van Genesen, S. T., Slingsby, C., and Lubsen, N. H. (2006) In vivo heteromers formation. Expression of soluble beta A4-crystallin requires coexpression of a heteromer partner. *FEBS J. 272*, 3172–3182.
26. Liu, B. F., Anbarasu, K., and Liang, J. J. (2007) Confocal fluorescence resonance energy transfer microscopy study of protein-protein interactions of lens crystallins in living cells. *Mol. Vision 13*, 854–861.

27. Basak, A., Bateman, O., Slingsby, C., Pande, A., Asherie, N., Ogun, O., Benedeck, G. B., and Pande, J. (2003) High-resolution X-ray crystal structures of human γD crystallin (1.25 Å) and the R58H mutant (1.15 Å) associated with aculeiform cataract. *J. Mol. Biol. 328*, 1137–1147.

28. Van Montfort, R. A., Bateman, O. A., Lubsen, N. H., and Slingsby, C. (2003) Crystal structure of truncated human βB1-crystallin. *Protein Sci. 12*, 2606–2612.

29. Kim, Y. H., Kapfer, D. M., Boekhorst, J., Lubsen, N. H., Bachinger, H. P., Shearer, T. R., David, L. L., Feix, J. B., and Lampi, K. J. (2002) Deamidation, but not truncation, decreases the urea stability of a lens structural protein, βB1-crystallin. *Biochemistry 41*, 14076–14084.

30. Slingsby, C., and Bateman, O. A. (1990) Quternary interactions in eye lens beta-crystallins:basic and acidic crystallins favor heterologous association. *Biochemistry 29*, 6592–6599.

31. Liu, B.-F., and Liang, J. J.-N. (2006) Domain interaction sites of human lens βB2-crystallin. *J. Biol. Chem. 281*, 2674–2630.

32. Descamp, F. J., Martens, E., Proost, P., Starckx, S., Van den Steen, P. E., Damme, J. V., and Opdenakker, G. (2004) Gelatinase B/matrix metalloproteinase-9 provokes cataract by cleaving lens βB1-crystallin. *FASEB J. 19*, 29–35.

33. Liu, B.-F., and Liang, J. J.-N. (2005) Interaction and biophysical properties of human lens Q155* βB2-crystallin mutant. *Mol. Vision 11*, 321–327.

34. Cohen, D., Bar-Yosef, U., Levy, J., Gradstein, L., Belfair, N., Ofir, R., Joshua, S., Lifshitz, T., Carmi, R., and Birk, O. S. (2007) Homozygous CRYBB1 deletion mutation underlies autosomal recessive congenital cataract. *Invest. Ophthalmol. Visual Sci. 48*, 2208–2213.